

ADVANCES IN FOREST FIRE RESEARCH

2022

Edited by
**DOMINGOS XAVIER VIEGAS
LUÍS MÁRIO RIBEIRO**

Fire propagation from surface to canopy on ornamental species under wind in laboratory conditions

Anthony Streit ¹; Bruno Guillaume ^{*1}; Bertrand Girardin ¹; Lucas Terrei ²; Anthony Collin ²; Alexis Marchand ³

¹ *Efectis France, Saint Aubin, France, {bruno.guillaume@efectis.com}*

² *LEMTA, Université de Lorraine, CNRS, Vandoeuvre-lès-Nancy, France*

³ *SCALIAN, Rennes, France*

**Corresponding author*

Keywords

Wildfires at Urban Interface, Fire propagation in parcels and structures, Wind-driven laboratory tests, WUI numerical modelling

Abstract

Fires in wildland-urban interfaces (WUIs) are resulting from intertwined physical processes at different scales: landscape, settlement, parcel, building and material (Vacca et al., 2020) and are causing growing damage worldwide in context of climate change and large urban sprawl.

The significant damage caused by these fires requires effective reinforcement of the resistance of structures and parcels against exposure to fire. Recent methodologies (Vacca et al., 2020 ; Benichou et al., 2021; Maranghides et al., 2022) have emphasised the need to look at these objectives by considering the spatial relationships between fuels, exposures and building resistance, in the perspective of a fire propagating in WUI according to so-called “fire pathways”. At parcel scale, the fire pathways often involve ornamental vegetation, that highly raises the damaging potential of the wildfire, this vegetation being at short distance to the structures and having a comparable size with buildings. Horizontal and vertical discontinuities in this vegetation do largely impact the exposure (Cohen, 2008) and installing such discontinuities is becoming part of the protection regulation against wildfires in different countries (Maranghides et al., 2022).

While the impact of embers has been extensively studied in the Insurance Institute for Business and Home Safety (IBHS) facilities (Manzello and Suzuki, 2014; Suzuki and Manzello, 2020), the effect of the fuel discontinuities on the reduction of thermal attack when approaching the building has been poorly addressed. This study aims at simulating in laboratory conditions a moving fire front pushed by wind and propagating from the surface to a canopy of ornamental vegetation, with fuel discontinuities. The experimental setup is composed of a fire lit in a surface excelsior fuelbed, propagating to a nearby vertical ornamental structure (excelsior and cypress) exposed to controlled high wind exposure (up to 3 m/s). The work is completed by a comparison of numerical modelling between the WFDS and FDS models.

The first steps of this study are shown here, showing a coherent sensitivity of the rate of spread to fuelbed width and fuelbed load, and showing the ability of WFDS and FDS to reasonably reproduce this rate of spread. The ability of FDS to propagate to an isolated vertical tree with the same modelling processes is also well established.

1. Introduction

Significant efforts have been made to understand the development and expansion of fires at the wildland-urban interface (WUI) (Cohen, 2008; Vacca et al., 2020), showing how the nearest combustible elements to the building are crucial for the propagation of the fire to the building. On the other hand, tree canopy fire contamination in native forests have independently been subject to various studies (Rothermel, 1991; Fernandes et al., 2009).

At homeowner scale, ornamental vegetation (isolated garden trees, hedges, climbing plants, ...) strongly enhances the danger coming initially from the native forest. In most tests and numerical simulations of WUI fires, these elements, located between the native forest and the building, are generally not represented. However, if represented they burn under very low wind conditions (Suzuki and Manzello, 2020; Li et al., 2021; Di Cristina et al., 2021), though in real fires (particularly true in South-East of France), fires in these ornamental elements occur under very gusty and chaotic wind conditions.

This study aims at experimentally reproducing a surface fire (excelsior fuelbed) propagating to a nearby vertical ornamental structure (excelsior and cypress), under high wind exposure (3 m/s) in the laboratory (*i.e.* at reduced scale). Additionally, a numerical setup composed of the models WFDS/FDS is used to compare and validate the codes against the experimental data.

This contribution describes the first steps of this study: the first section describes how zero-wind surface fire experimental data are generated to evaluate the sensitivity of Rate Of Spread (ROS) to fuel load and fuel width. The second section describes the setup of FDS and WFDS models that will be used in the entire study. Then results of some nominal and intermediate model configurations are presented. The last section is dedicated to the intermediate conclusions and to introduce the next steps of the study.

2. Calibration of the zero-wind surface fire in the experimental setup

The first step consisted in evaluating the ROS of a surface fire under zero-wind condition, in order to gain in reproducibility of surface fires for the full experimental setup. This is a first validation before developing the full experimental setup composed of a surface fire propagating to an ornamental vegetation under high wind exposure (Figure 1b). 85 experiments were performed with zero-wind surface fires (Marchand et al., 2014, 2019). They were carried out on excelsior as fuelbed (Figure 1a) and the sensitivity to fuelbed width and fuelbed load was investigated. The combustible material was fully characterised in a previous work by Marchand et al. (2019). The first 45 experiments were conducted with a constant vegetation load (0.5 kg/m²) and with fuelbed width ranging from 25 cm to 3.5 m. The excelsior was spread onto the table in order not to exceed a maximum average height of 8.5 cm. The fire was ignited on a line along the whole bed width. The last 40 fire tests were conducted with a constant fuelbed width of 2 m and with a fuel load ranging from 0.1 kg/m² to 1 kg/m². Visible cameras combined with image processing (Otsu algorithm) were used and a direct linear transformation (DLT) algorithm was developed in order to quantify fire behaviour properties (ROS, fire length, etc.).

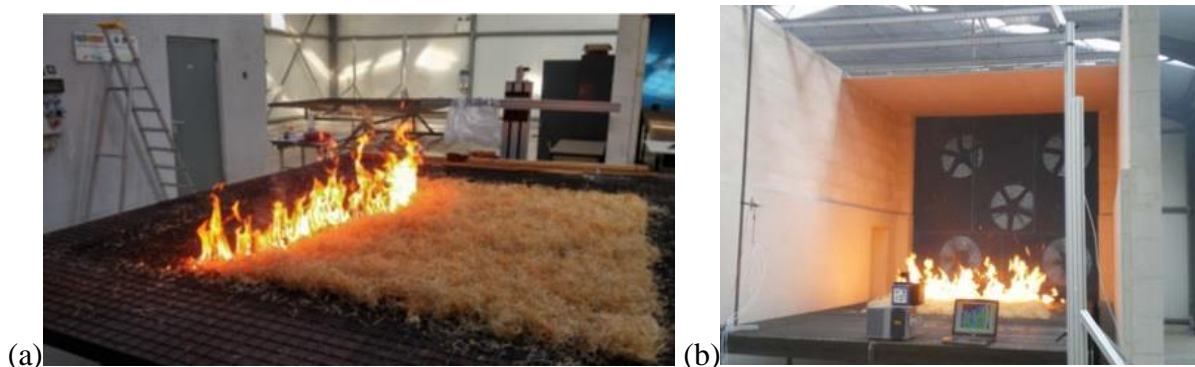


Figure 1 - Zero-wind fire spread test on the surface fuelbed, (b) View of the high wind exposure facility

A summary of main results is shown in Figure 2. For the sensitivity of ROS to fuelbed width, ROS is shown to increase at low values of fuel bed width and seems to reach a constant value of about 1.5 cm/s for a 2 m fuel bed width and beyond. In such configurations, the fire fronts are near-parabolic, but the front curvature varies with the line width and the rate of spread is also affected. For the sensitivity to fuelbed load, ROS is shown to globally increase with fuel loads from 0.3 cm/s for the lowest load to 2.6 cm/s in average for the highest load. The repeatability of tests showed discrepancy up to 0.5 cm/s as compared to the average value that can be significant but explained by ambient conditions (different seasons and ambient conditions).

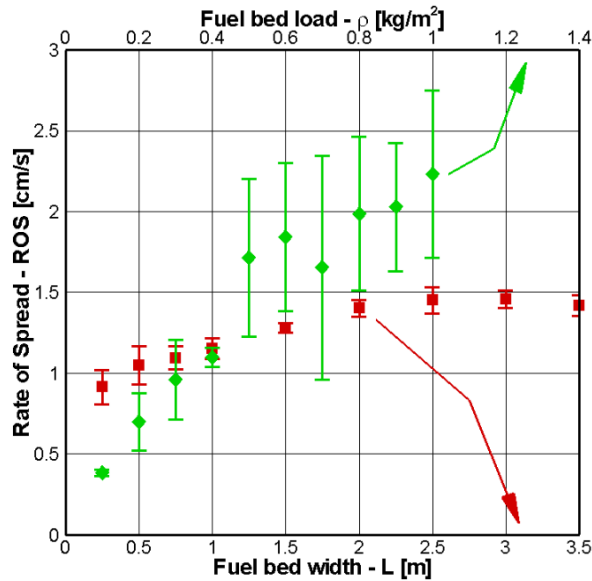


Figure 2 - Distribution in the 85 experiments of the rate of spread as a function of fuelbed width (red colour) for a constant vegetation load of 0.5 kg/m^2 and as a function of fuelbed load (green colour) for a constant fuelbed width set at 2 m.

3. Wind-driven surface fire experiments

A second step consisted in evaluating the ROS of the wind-driven surface fire. Five different wind fans of the “wind wall” were activated with the same constant frequency in each individual experiment. The wind measurements collocated to the fans and at different horizontal distances from the fans, at 0 m and 1 m ground heights are shown in Figure 3. The wind at $z = 0 \text{ m}$ ground height is more affected by the distance to the fans than the wind at $z = 1 \text{ m}$. All fan frequencies cannot be used when burning the vegetation since above 30 Hz the excelsior is heavily washed from the table by the wind.

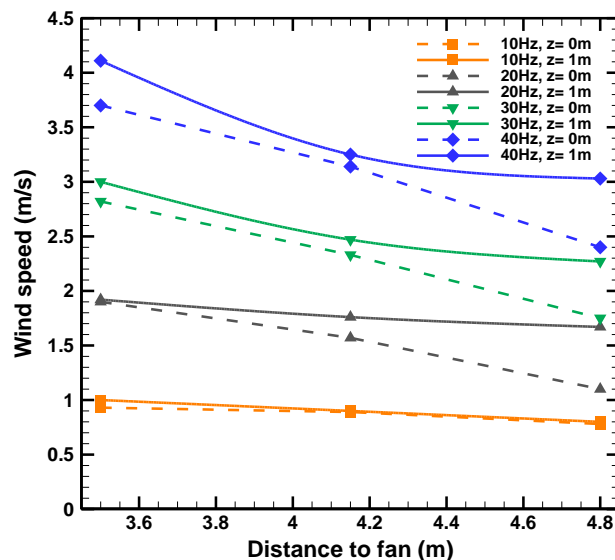


Figure 3 – Wind speed with horizontal distance to the fans, and at two different ground heights ($z=0\text{m}$ and $z=1\text{m}$)

Different tests of excelsior burning under different wind speeds have been conducted at two different vegetation loads, set at 0.23 kg/m^2 and 0.4 kg/m^2 . The excelsior fuelbed was positioned at a distance of 1.3 m from the fans.

As shown on Figure 4, the ROS exhibits a strong increase when going from zero-wind to 0.88 m/s wind speed, with a multiplication of ROS by 4 for the 0.23 kg/m² case and by 6 for the 0.4 kg/m² case. Then a plateau of ROS is observed between 0.88 m/s wind speed and 1.9m/s wind speed and finally another strong ROS increase occurs when reaching 2.4 m/s wind speed.

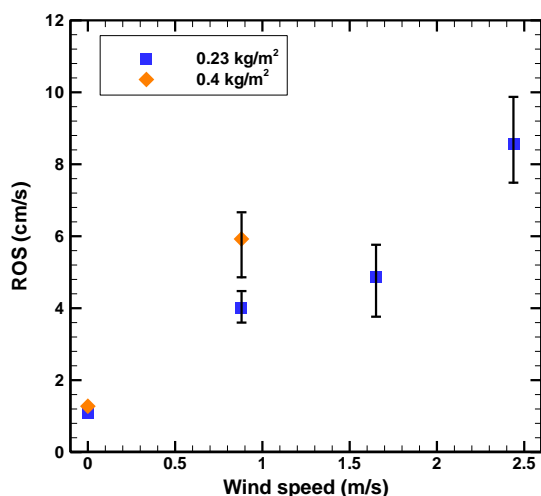


Figure 4 – Rates of spread in function of the wind speed for two different loads (0.2 kg/m² and 0.4 kg/m²)

4. Calibration of the surface and canopy fires, with wind, in the experimental setup

Finally, the full experimental setup composed of a surface fire propagating from excelsior to an ornamental vegetation in form of a very thin hedge, with and without wind exposure, has been tested, with the same objective of monitoring ROS.

Two types of vegetation were sampled to constitute the hedge: cypress and oleander. This vegetation was arranged with equal fuel load on a vertical mesh of 1 m large and 1.5 m height, by intertwining the branches with the fine diameter coarse galvanized steel mesh, which has the advantage of preventing the vegetation from collapsing when burning. A simple evaluation showed that the very fine diameter of the mesh would not modify significantly the fire power or the ROS over the hedge. Same fuel load was imposed on the entire mesh with respectively about 1.2 kg/m² and 4 cm depth for cypress and about 1.2 kg/m² and 6 cm depth for oleander, collected in gardens and let drying for a minimum of 15 days. Size distribution of <2mm, 2-4 mm, and 4-6 mm diameters were found for cypress of 34.7 %, 55.1%, and 10.2 %. Size distribution of 2-4 mm, 4-6 mm, and 6-8 mm diameters were found for oleander of 48 %, 44 %, and 8 %. The Figure 5 shows cypress and oleander branches and the bulk density evaluation by tube test.



Figure 5 – Property measurements: (left) oleander weighting, (middle) cypress branches clustering for size distribution evaluation, (right) cypress bulk density evaluation

The Fuel Moisture Content (FMC) was sampled 1 day before the experiment. FMC of cypress was about 23.8 % on dry matter basis. FMC of oleander was about 10.7 %. The FMC for cypress has been measured 15 times with a SD (standard deviation) of 9.6%, 6 times with a SD of 1.3% for oleander, and 5 times with a SD of 0.7% for excelsior. For ROS measurements, a total of 8 thermocouples (TCs) were vertically-positioned, 4 being vertically aligned along the middle of the hedge and 4 others vertically aligned along the exterior side of the

hedge. Each TC is 50 cm distant from another, covering a distance of 0.1 m to 1.6 m over the table. Two visible cameras were also placed, one at the back of the hedge and another one on the side.

A series of 2 experiments were conducted with cypress under zero-wind conditions, while 1 experiment was conducted with cypress under 10 Hz wind conditions (around 0.88 m/s) (outputs not shown here), and 2 experiments were conducted with oleander under zero-wind conditions. Under zero-wind conditions, the fire contaminates the hedge only after the excelsior fire has arrived very close to the foot of the hedge (Figure 6).



Figure 6 – Fire contaminating from excelsior fire to the hedge under zero-wind conditions, (upper) for cypress and (lower) for oleander. Propagation visualized in 5 phases (from left to right): excelsior fire approaches, excelsior fire at the foot of the hege (reference time $t=0s$), fire at maximum development in the hedge, fire largely decreasing, fire in extinction phase

ROS of the fire in the hedge was quantitatively extracted from the vertically-positioned TCs under zero-wind conditions, but the oscillatory flames did contaminate the vertical sensors in an erratic sequence (with higher TCs contaminated prior to lower TCs), preventing from getting the ROS this way. The measurements from visible cameras revealed a robust way to measure ROS, the imagery being preliminarily distance-referenced (Figure 7). Cypress fire exhibited ROS values respectively between 35 cm/s and 43 cm/s under zero-wind condition, and 55 cm/s under 10 Hz wind condition. The oleander exhibited ROS values between 22 and 24 cm/s under zero-wind condition. More experiments have been scheduled to gain statistical robustness of these results. Additionally the calibration of the WFDS and FDS models is in ongoing process on these data.

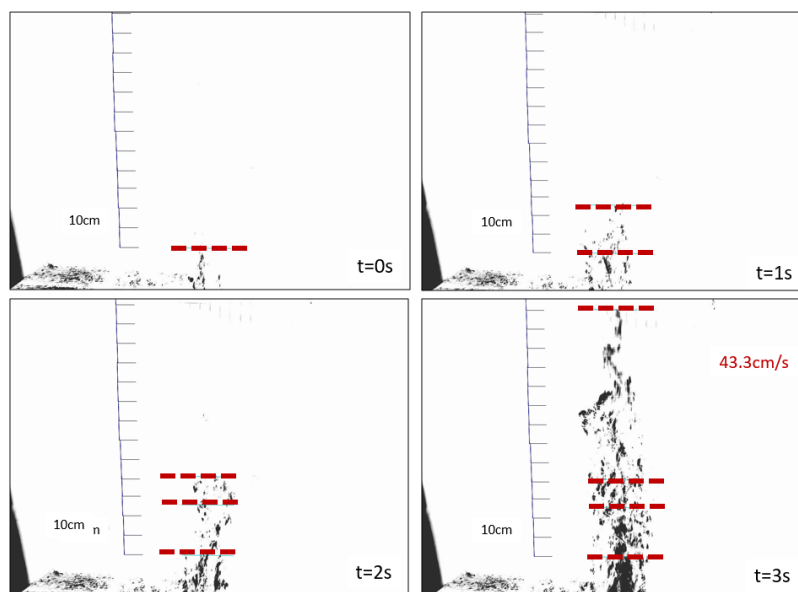


Figure 7 – Zero-wind condition cypress ROS measured by manual interpretation on distance-referenced thermal camera imagery

5. Numerical setup

The two versions of “FDS” (Fire Dynamic Simulator), the classical FDS and its WFDS derivation (Wildland Fire Dynamic Simulator) are used in this study. Each numerical model has its own parameters to represent the vegetation fuel and should be calibrated. In the literature, grid resolution to reproduce laboratory “forest fire” experiments may vary from 2 cm (Morandini et al. (2019) for rockrose shrubs) or 5 cm (Wickramasinghe et al. (2020) for Douglas fir) and up to 10 cm (Mell et al. (2009) for the same Douglas fir).

The WFDS model in 7.6 version is used here with a uniform spatial resolution along the three directions of $\Delta = 2$ cm. The linear pyrolysis model is employed in WFDS.

The Fire Dynamic Simulator (FDS) in version 6.7.5 is used here with either (1) a uniform spatial resolution along the three directions of $\Delta = 2$ cm, or (2) with $\Delta x = \Delta z = 1$ cm and $\Delta y = 2$ cm. The pyrolysis and char oxidation processes are driven by an Arrhenius model.

6. Nominal WFDS and FDS calibration on the intermediate setup of a zero-wind surface fire

The tests modelled with WFDS for the zero-wind surface fire require to attribute values to eight key parameters of the pyrolysis model: the maximum value allowed for the MLR [MLRmax in $\text{kg}/\text{m}^3/\text{s}$], the bulk density of vegetation [ρ_{bulk} in kg/m^3], the density of vegetative fuel [ρ in kg/m^3], the surface-to-volume ratio of vegetation [σ in $1/\text{m}$], the moisture fraction H_u in %wt (calculated on a dry mass basis), the fraction of dry virgin vegetation that becomes char τ_{char} (in %wt), the heat of combustion [ΔH_r in kJ/kg] and an adimensional multiplicative drag coefficient C_f .

Raw values of these parameters have been previously obtained by Marchand et al. (2019) and are presented in Table 1. Simulations were made to determine the ROS evolution as a function of the fuelbed width for a $0.5 \text{ kg}/\text{m}^2$ vegetation load using these raw values as input data. Despite that, the global trend is well captured as the ROS increases with the fuel bed width, these simulations exhibited a strong underestimation (60 % differences with the experimental data). Therefore, these values have been fitted: a local sensitivity analysis revealed that MLRmax and ΔH_r were the most significantly sensitive parameters for the ROS predicted by the WFDS model. An identification algorithm (Particle Swarm Optimisation method according to Kennedy and Eberhart (1995)) was then used to identify the best values for these two input parameters, keeping all others at their initial experimental values. As presented in Figure 8, with these new parameters, the numerical trend of ROS with fuelbed width is in a good agreement with the experimental data.

The tests modelled with FDS for the same test configuration require to attribute values to several parameters driving the thermal decomposition and char oxidation. More details about model formulation can be found in Mell et al. (2009), Perez-Ramirez et al. (2017) and Morandini et al. (2019) or Porterie et al. (2009). Most of the parameters are extracted from these previous studies. Namely, the parameters describing the dehydration of the vegetation are taken as $E_{H_2O} = 5800K$, $A_{H_2O} = 6 \times 10^5 s^{-1} K^{-1/2}$ and $\Delta H_{H_2O} = 2.2596 \times 10^3 J.kg^{-1}$ (endothermic). The parameters describing the decomposition of the vegetation into combustible fuel are $E_{pyr} = 7250K$, $A_{pyr} = 3.63 \times 10^4 s^{-1}$ and $\Delta H_{pyr} = 1.297 \times 10^3 J.kg^{-1}$ (endothermic). The latter parameter is the only parameter that is not extracted from Perez-Ramirez et al. (2017) or Porterie et al. (2009), its value was fitted so the predicted ROS under zero-wind condition was similar to the experimental one with a fuelbed of $0.5 kg/m^2$ and a fuel width of $0.25 m$. The char oxidation model and its inputs was extracted from Perez-Ramirez et al. (2017). Namely, the following parameters were used in our study : $E_{char} = 9000K$, $A_{char} = 430 m.s^{-1}$ and $\Delta H_{pyr} = 32 \times 10^3 J.kg^{-1}$ (exothermic).

Table 1 -Input parameters used for WFDS: comparison between raw experimental values and fitted optimised values

Features	Initial experimental values	Fitted Optimal values
MLRmax [$kg/m^3/s$]	0.22	0.43
ρ_{bulk} [kg/m^3]		5.55
ρ [kg/m^3]		519
σ [$1/m$]		14 600
Hu [-]		0.12
τ_{char} [-]		0.31
ΔHr [kJ/kg]	16 480	14 497
Cf [-]		0.375

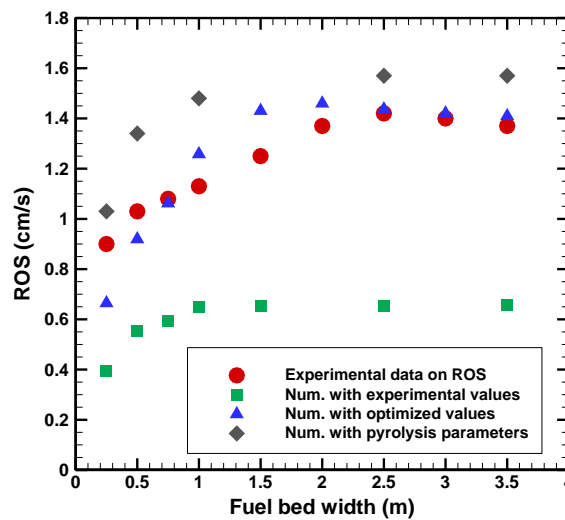


Figure 8 - Results of the two sets of WFDS simulations of ROS, with raw experimental values of the pyrolysis model parameters, and fitted optimal values

Simulations of FDS conducted with too low fuel loads ($0.23 kg/m^2$) did exhibit no propagation, and calibrating different char oxidation parameters did not change this limiting model behavior. As seen in next section, when using a value of $0.3 kg/m^2$ as in Meerpoel-Pietri et al. (2022) did not exhibit this problem.

7. Nominal FDS simulation on the intermediate setup of a wind-driven surface fire

The configuration of Figure 4 is simulated using the FDS model, using a fuel load of $0.5 kg/m^2$. The model shows a coherent tendency in respect to the observations, with a lower increase of ROS with wind. More experiments at $0.4 kg/m^2$ with wind have been scheduled to gain statistical robustness of these results, to be compared with simulation at $0.4 kg/m^2$.

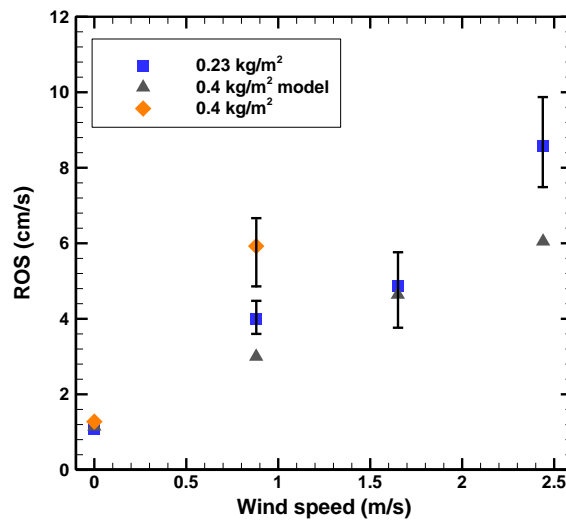
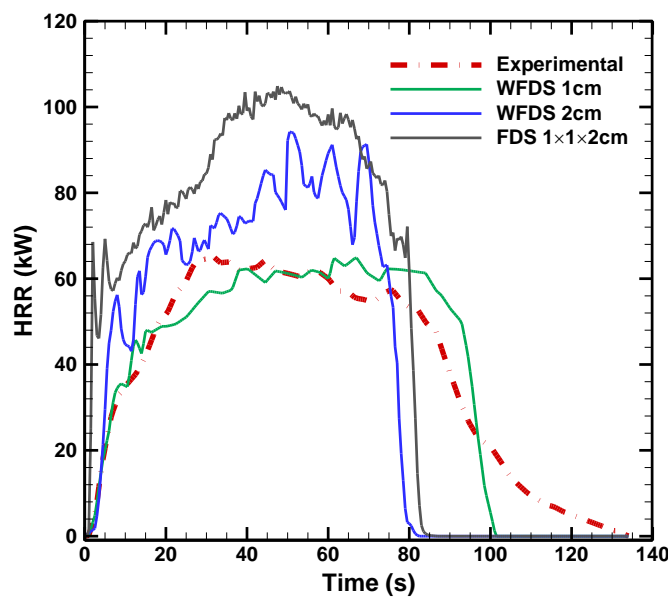


Figure 9 – Comparison of rates of spread varied with wind intensity, for two different loads (0.2 kg/m² and 0.4 kg/m²) for the experiments, and for one load (0.5 kg/m²) for the model

8. Nominal FDS simulations in similar setups

A simulation setup is used to illustrate the ability of FDS model to reproduce a zero-wind surface fire, extracted from Meerpoel-Pietri et al. (2022) referred hereafter as MP2022, with additional 20 % slope of the fuelbed. The fuelbed is also there composed of excelsior. The configuration from MP2022 as well as the input values given by the authors for the Arrhenius pyrolysis model are used within the FDS model, while the authors used the WFDS model.

As shown in Figure 10, the FDS outputs have a very similar intensity curve as the WFDS at 2 cm resolution from MP2022, while being globally 22 % higher in intensity in the period between 5 s and 77 s. The difference in terms of intensity may be explained by the difference of the two codes. However, the ROS is coherent with the WFDS results and with the experimental data.



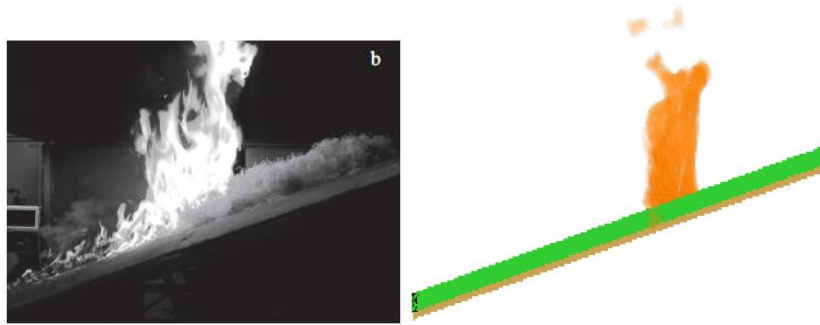


Figure 10. (upper row): Comparison of the intensity-time curves: the WFDS 1 cm and 2 cm and the experimental data are taken from MP2022 while the FDS is from current study, (lower row): Comparison in side view along the full slope of the observed (left) and modelled (right) flame height at timestep 51 s (source: observed flame photo is from Meerpoel Pietri et al. (2022))

A second similar setup as the full ornamental vegetation setup of this study is the single-tree canopy fire under zero wind provided by Mell et al. (2009), referred hereafter as M2009. The Mass Loss Rates (MLR) are calculated with FDS in this study for two different grid resolution, 10 cm and 25 cm, together with two different pyrolysis schemes: Arrhenius (same scheme as in the previous nominal zero-wind surface fire test) and simplified Arrhenius (scheme from older FDS versions). As shown in Figure 11 for a 5 m tree, the M2009 WFDS simulation is the closest to the experimental data, but all simulations from our study vary here only with a delay of less than 5 seconds in the peak MLR value, and with less than 20 % difference in peak value.

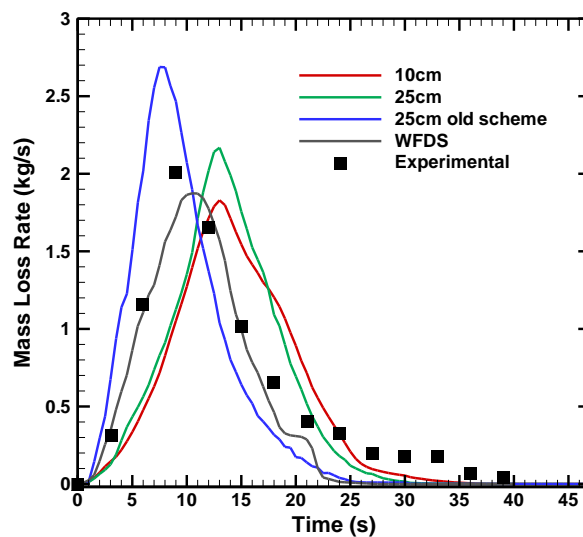


Figure 11 - Time evolution of MLR in current FDS version with both pyrolysis schemes and both resolutions (10 cm and 25 cm), compared with the Mell et al. (2009) experiment data and numerical WFDS outputs

These nominal simulations of FDS based on current state model should be confronted with observations of next coming surface and canopy fire tests in the study.

9. Conclusions

Based on experimental data on zero-wind surface fire propagation, this contribution showed promising results on the ability of WFDS and FDS to reproduce well the fire front behaviour. Moreover, the ability of FDS to propagate to an isolated vertical tree with the same modelling processes is also presented and validated.

A new experimental setup allowing simulating a scenario of fire contamination from the surface to an ornamental vegetation, under high wind conditions, is in ongoing development. It involves a surface fire

scenario, represented by a fire in Excelsior, which contaminates an ornamental vegetation. Some targeted nominal intercomparisons with the WFDS and FDS models will be presented in the final contribution. This new experimental setup will allow in a coming future to evaluate the impact of vertical discontinuities (low branches position of the ornamental vegetation), as well as effect of wind intermittency.

10. References

- Benichou N., Adelzadeh M., Singh J., Gomaa I., Elsagan N., Kinateder M., Ma C., Gaur A., Bwalya A., and Sultan M. (2021). National Guide for Wildland-Urban Interface Fires. National Research Council Canada: Ottawa, ON. 192 pp
- Cohen J (2008) The wildland-urban interface fire problem: A consequence of the fire exclusion paradigm. *Forest History Today*. Fall: 20-26.
- Di Cristina G., Kozhumal S., Simeoni A., Skowronski N., Rangwala A.; Im, S.-K. (2021). Forced convection fire spread along wooden dowel array. *Fire Safety Journal*. 120: 103090. <https://doi.org/10.1016/j.firesaf.2020.103090>.
- Fernandes P.-M. (2009). Combining forest structure data and fuel modelling to classify fire hazard in Portugal. *Annals of Forest Science*, Springer Nature (since 2011)/EDP Science (until 2010), 66 (4).
- Kennedy J. and Eberhart R. (1995) « *Particle swarm optimization* », *IEEE International Conference on Neural Networks*, 1995. *Proceedings*, vol. 4, p. 1942–1948.
- Li B. , Ding L. ,Simeoni A. , Ji J. ,Wan H.,Yu L. (2021) Numerical investigation of the flow characteristics around two tandem propane fires in a windy environment, *Fuel*, 286, 119344.
- Manzello L. and Suzuki S. (2014), Exposing Wood Decking Assemblies to Continuous Wind-Driven Firebrand Showers, *Fire Safety Science* 11: 1339-1352.
- Maranghides A., Link E., Nazare S., Hawks S., McDougald J, Quarles S., Gorham D. (2022) WUI Structure/ Parcel/ Community fire hazard mitigation methodology, NIST Technical Note 1600. National Institute of Standards and Technology, Gaithersburg, MD.
- Marchand A., Trevisan N., Collin A. and Boulet P. Fire propagation, *Cellular automaton model, Fire front width effect, Radiative transfer*, in *Advances in forest fire research*, Imprensa da Universidade de Coimbra, 2014.
- Marchand A., Ferrière S., Collin A., Boulet P. Acem Z., Demeurie F. and Morel J.-Y. Vegetation fire spread database : 85 wood wool shaving experiments at laboratory scale. *Fire Safety Journal*, Vol. 109, 102870, 2019.
- Suzuki S. and S.L. Manzello (2020) Investigating coupled effect of radiative heat flux and firebrand shower on ignition of fuel beds, *Fire Technology*.
- Maranghides, A. , Link, E. , Nazare, S. , Hawks, S. , McDougald, J. , Quarles, S. and Gorham, D. (2022), WUI Structure/Parcel/Community Fire Hazard Mitigation Methodology, Technical Note (NIST TN), National Institute of Standards and Technology, Gaithersburg, MD, [online], <https://doi.org/10.6028/NIST.TN.2205>,
- McGrattan, K.B., Klein, B., Hostikka, S., and Floyd, J (2008). *Fire Dynamics Simulator Users Guide*. NIST Special Publication 1019-5, National Institute of Standards and Technology, U.S. Department of Commerce, Gaithersburg, MD.
- Meerpoel-Pietri K., Tihay-Felicelli V., Graziani A.,Santoni P.-A., Morandini F., Perez-Ramirez Y., Bosseur F.,Barboni T., Sánchez-Monroy X., Mell W. (2022): Modeling with WFDS Combustion Dynamics of Ornamental Vegetation Structures at WUI: Focus on the Burning of a Hedge at Laboratory Scale, *Combustion Science and Technology*, DOI: 10.1080/00102202.2021.2019235
- Mell W, Jenkins MA, Gould J, Cheney P (2007) A physics based approach to modeling grassland fires. 2007. *International Journal of Wildland fire*. 16(1): 1-22.
- Mell W., Maranghides A., McDermott R., and Manzello S.L. (2009) Numerical simulation and experiments of burning douglas fire trees, *Combustion and Flame*, vol. 156, no. 10, pp. 2023–2041.
- Morandini, F.; Santoni, P.A.; Tramonì, J.B.; Mell, W.E. (2019) Experimental investigation of flammability and numerical study of combustion of shrub of rockrose under severe drought conditions. *Fire Safety Journal*. 108: 102836
- Perez-Ramirez Y., Mell W.E., Santoni P.-A., Tramonì J.-B., Bosseur F., 2017, Examination of WFDS in Modeling Spreading Fires in a Furniture Calorimeter. *Fire Technology*, Springer Verlag, 2017, 53 (5), pp.1795-1832.

- Porterie B., J. L. Consalvi, A. Kaiss & J. C. Loraud (2005) Predicting Wildland fire behavior and emissions using a fine scale physical model, *Numerical Heat Transfer, Part A: Applications*, 47:6, 571-591
- Rothermel, Richard C. 1991. Predicting behaviour and size of crown fires in the northern Rocky Mountains. Res. Pap. INT-RP-438. Ogden, UT: U.S. Department of Agriculture, Forest Service, Intermountain Research Station. 46 p.
- Vacca, P.; Pastor, E.; Planas, E.; Caballero, D. 2020 WUI I fire risk mitigation in Europe: A performance-based design approach at home-owner level, *Journal of safety science and resilience*, 1 (2), p. 97-105
- Vanella M, McGrattan K, McDermott R, Forney G, Mell W, Gissi E, Fiorucci P. A (2021) Multi-Fidelity Framework for Wildland Fire Behavior Simulations over Complex Terrain. *Atmosphere*. 12(2):273.
- Wickramasinghe A, Khan N and Moinuddin K (2020) Physics-based simulation of firebrand and heat flux on structures in the context of AS3959. Project Report. Bushfire and Natural Hazard CRC, Melbourne, Victoria